

## *Invited Lecture*

# **ASSESSING LIQUEFACTION IN GRAVELLY SOILS BASED ON FIELD CASE HISTORIES**

Kyle Rollins <sup>(1)</sup> and Jashod Roy <sup>(2)</sup>

<sup>(1)</sup> Professor, Brigham Young University, [rollinsk@byu.edu](mailto:rollinsk@byu.edu)

<sup>(2)</sup> Staff Engineer, Kiewit Engineering, [Jashod.Roy@gmail.com](mailto:Jashod.Roy@gmail.com)

## **Abstract**

Gravelly soils have liquefied at multiple sites in at least 27 earthquakes over the past 130 years. These gravels typically contain more than 25% sand which lowers the permeability and makes them susceptible to liquefaction. Developing a reliable, cost-effective liquefaction triggering procedure for gravelly soils has been a challenge for geotechnical engineers. Typical SPT- or CPT-based correlations can be affected by large-size gravel particles and can lead to erroneous results. To deal with these problems, we have developed liquefaction triggering curves for gravelly soils based on (1) shear wave velocity ( $V_s$ ) and (2) a large diameter cone penetrometer. With a cone diameter of 74 mm, the Chinese Dynamic Cone Penetration Test (DPT) is superior to smaller penetrometers and can be economically performed with conventional drilling equipment. Using logistic regression analysis, the DPT has been directly correlated to liquefaction resistance at sites where gravels did and did not liquefy in past earthquakes. Probabilistic liquefaction resistance curves were developed based on 137 data points from 10 different earthquakes in seven countries. Using a similar data set, probabilistic liquefaction triggering curves were also developed based on  $V_s$  measurements in gravelly soils. The  $V_s$ -based liquefaction triggering curves for gravels shift to the right relative to similar curves based on sands. New magnitude scaling factor ( $MSF$ ) curves have also been developed specifically for gravel liquefaction which were found to be reasonably consistent with previous curves for sand.

*Keywords: Gravels, Liquefaction, Case Histories, Shear Wave Velocity, Dynamic Cone Penetration Test, DPT*

## **1. Introduction**

Liquefaction of loose saturated granular soils results in significant damage to civil infrastructure such as buildings, bridges, roadways, pipelines, and ports in nearly every earthquake. Liquefaction and the resulting loss of shear strength can lead to landslides, lateral spreading, loss of vertical and lateral bearing support for foundations, and excessive foundation settlement and rotation. Direct and indirect economic losses resulting from liquefaction are substantial costs to society. A significant number of gravel liquefaction case histories have occurred during more than 20 earthquake events over the past 130 years, as shown in Table 1. Assessing the potential for liquefaction of gravelly soils in a reliable, cost-effective manner has always posed a great challenge for geotechnical engineers and researchers. Liquefaction assessment is particularly important for older dams that were constructed on gravelly soil foundations or with poorly compacted gravel shells before the potential for liquefaction in gravels was recognized. Likewise, many ports around the world were constructed of gravelly soils or rockfill which was believed to be immune to liquefaction. For these projects, assessing the potential for liquefaction and determining appropriate remedial measures are often multi-million-dollar decisions. These decisions involve both life-safety and regional economic issues. Over the past 15 years, gravel liquefaction has caused significant damage to ports in Greece, Chile, Ecuador, and New Zealand. Besides these large projects, gravel liquefaction must be routinely considered for a myriad of small to medium projects throughout the world.

Table 1 - Case histories involving liquefaction of gravelly soil

| Earthquake                | Year | M <sub>w</sub> | Reference    |
|---------------------------|------|----------------|--------------|
| Mino-Owari, Japan         | 1891 | 7.9            | [1]          |
| San Francisco, California | 1906 | 8.2            | [2]          |
| Messina, Italy            | 1908 | 7.1            | [3]          |
| Fukui, Japan              | 1948 | 7.3            | [4]          |
| Alaska, USA               | 1964 | 9.2            | [5,6]        |
| Hatching, China           | 1975 | 7.3            | [7]          |
| Tangshan, China           | 1976 | 7.8            | [8]          |
| Friuli, Italy             | 1976 | 6.4            | [9, 10, 11]  |
| Miyagiken-Oki, Japan      | 1978 | 7.4            | [1]          |
| Borah Peak, Idaho, USA    | 1985 | 6.9            | [12, 13, 14] |
| Armenia                   | 1988 | 6.8            | [15]         |
| Limon, Costa Rica         | 1991 | 7.7            | [16]         |
| Roermond, Netherlands     | 1992 | 5.8            | [17]         |
| Hokkaido, Japan           | 1993 | 7.8            | [18]         |
| Kobe, Japan               | 1995 | 7.2            | [19]         |
| Chi-Chi, Taiwan           | 1999 | 7.8            | [20]         |
| Wenchuan, China           | 2008 | 7.9            | [21]         |
| Tohoku, Japan             | 2010 | 9.0            | [22]         |
| Cephalonia Is., Greece    | 2012 | 6.1            | [23, 24]     |
| Iquique, Chile            | 2014 | 8.2            | [25, 26]     |
| Muisne, Ecuador           | 2016 | 7.8            | [27]         |
| Kaikora, New Zealand      | 2016 | 7.8            | [28]         |
| Durres, Albania           | 2019 | 6.4            | [29]         |
| Petrinja, Croatia         | 2020 | 6.4            | [30]         |

## 2. Penetration Testing Approaches

Typical laboratory investigation techniques have generally proven to be ineffective for characterizing gravelly soil due to the cost and difficulty of extracting undisturbed sample from gravelly deposits [21]. In addition, the large particle size of gravels can lead to artificially high penetration resistance values from traditional in situ tests such as the cone penetrometer (CPT) test and the Standard Penetration (SPT) test [31]. The 168 mm diameter Becker Penetration Test (BPT) [32, 33] reduces the potential for artificially high penetration values; however, this method is relatively expensive and is not available outside of North America. In addition, the method requires a correlation between the BPT blow count and the SPT blow count which leads to greater uncertainty relative to methods that are directly correlated with field liquefaction resistance.

As another approach for gravelly soils, Chinese engineers in the Chengdu region, faced with widespread gravel deposits, developed a Dynamic Cone Penetrometer (DPT) with a 74 mm diameter cone tip for site characterization. The methodology is a large-size implementation of the lightweight dynamic cone penetrometer that is used extensively for assessment of compaction of soils in pavement applications [34] and different cone geometries are also known as dynamic probing in Europe [35]. In the Chinese version of the DPT, the cone tip is driven continuously with a 120 kg hammer dropped from one meter and is capable of penetrating medium to dense gravel and cobbles. DPT soundings can be easily performed with conventional SPT drilling rigs or even simple tripod systems, making it viable worldwide. In contrast to the straight sides of the BPT, the cone tip tapers back to a 60 mm drill rod to reduce rod friction. At 74 mm, the DPT diameter is 50% larger than the SPT and 110% larger than a standard 10 cm<sup>2</sup> CPT; however, it is still 55% smaller than the BPT. Although the BPT provides the

largest diameter to particle size ratio of all tests, the DPT is superior to the SPT or CPT and could be a reasonable solution in many cases depending on the gravel size and percentage.

Based on field case histories of gravel liquefaction in the  $M_w$  7.9 Wenchuan earthquake, Cao et al. [21] developed probabilistic liquefaction triggering curves for gravels based on the DPT blow count. However, these curves are based on relatively few data points from one earthquake and a geologic profile consisting of a loose alluvial fan gravel layers overlain by a clay surface layer typically 2- to 4-m thick [21]. Because of the limited number of data points and the possibility of false negatives (sites where liquefaction may have occurred but did not produce surface manifestation), the individual triggering curves (85 to 15%) are spread apart. In contrast, more mature probabilistic liquefaction triggering curves for sands based on CPT [36] have more closely grouped probability curves because of the larger size of the data set. In addition, the Cao et al. [21] triggering curves were developed for a single event of  $M_w$  7.9 without incorporating any correction to the seismic demand by using the Magnitude Scaling Factor (*MSF*). Thus, applicability of these curves would become questionable for evaluating the liquefaction potential of gravelly soils for other seismic events of different Magnitude. Although existing *MSF* models developed for sand liquefaction [37] can be used, it is unclear whether they are appropriate for gravel liquefaction using the DPT. Therefore, it becomes crucial to add more case histories to the DPT database with different earthquake magnitudes and geologic settings and develop an improved DPT-based liquefaction triggering procedure and a gravel-based *MSF* curve.

### 3. Shear Wave Velocity Approaches

As an alternative to penetration resistance testing, in situ measurement of shear wave velocity ( $V_s$ ) is a popular way of characterizing the liquefaction resistance of soil deposits.  $V_s$  is a basic mechanical property of soil materials, directly related to the small strain shear modulus ( $G_0$ ), that is an essential parameter for performing soil-structure interaction analysis and liquefaction evaluation under earthquake loading. The use of  $V_s$  as a field index of liquefaction resistance is soundly based on the fact that both  $V_s$  and liquefaction resistance are similarly, but not proportionally, influenced by void ratio, effective confining stresses, stress history and geologic age [37]. In addition,  $V_s$  is considerably less sensitive to the problems of soil compression and reduced penetration resistance when fines are present, compared with SPT and CPT methods. Moreover,  $V_s$  requires only minor corrections for fines content (*FC*) at least for sands [38]. The primary advantage of the in-situ  $V_s$  approach is that testing can be performed at sites where borings are not possible, or the penetration test results may be unreliable. Hence,  $V_s$  measurement can be considered as a reliable and economical alternative to overcome the difficulties of penetration testing within gravelly strata.

The traditional methods of measuring  $V_s$  require a penetrometer or instrumented boreholes to measure the travel time of shear waves at various depths. A downhole test requires one borehole to measure the vertically propagating wave, while a cross-hole test requires at least two boreholes to directly measure the horizontally propagating wave [39]. These invasive test methods are usually quite expensive due to the cost of drilling, casing, and grouting boreholes. In the last two decades, some advanced non-invasive test methods (Spectral Analysis of Surface Waves (SASW) and Multichannel Analysis of Surface Wave (MASW) have been developed, which indirectly estimate the  $V_s$  through the surface wave dispersion characteristics of the ground [13, 38, 39]. These non-invasive test methods have significantly reduced the cost of in-situ  $V_s$  estimation and made soil exploration possible at sites where penetration is not possible or economically feasible.

Andrus and Stokoe [40] increased the population of  $V_s$  data by collecting a large database from locations around the world where both sandy and gravelly soils had liquefied in various seismic events. Based on this dataset, improved triggering curves were developed for sands and gravels for different *FC* percentages. The database of Andrus and Stokoe [40] only contained a limited number of data points where the  $V_{s1}$  was higher than 200 m/s even for gravelly soils. This is consistent with observations by Kokusho et al. [13] that loose gravels, even though well-graded, can exhibit shear wave velocities similar to those of loose sands. In contrast, the SPT- $V_s$  correlation by Ohta and Goto [41] and the

correlation by Rollins et al. [42] suggest a higher range of  $V_{s1}$  (230 m/s) for liquefiable Holocene gravels. Such variation of shear wave velocity in gravelly soils can be due to variations in gravel content, grain size distribution, and the relative density of the soil matrix [13, 43, 44, 45].

Cao et al. [46] developed probabilistic liquefaction triggering curves for gravels using logistic regression techniques based on  $V_s$  data collected from the Chengdu plain in China where gravel liquefaction took place during the 2008 Wenchuan earthquake. These curves are based on 47 data points (19 liquefaction and 28 no liquefaction points) that refer to a single earthquake and a similar geological environment [46]. Because of the limited number of data points and the possibility of false negatives (sites where liquefaction may have occurred but did not produce surface manifestation), the individual triggering curves (15% to 85%) are relatively far apart. In contrast,  $V_s$ -based probabilistic liquefaction triggering curves for sands [38] have more closely grouped probability curves because of the larger size of the data set. Moreover, the Cao et al. [46] triggering curves were developed for a single event of  $M_w$  7.9 without proposing any correction to the seismic demand for different earthquake magnitudes. Thus, the applicability of these curves becomes questionable for evaluating the liquefaction potential of gravelly soils for other seismic events of different magnitude. Although existing *MSF* models developed for sand liquefaction [37] can be used, it is unclear whether they are appropriate for gravel liquefaction assessment based on  $V_s$ . Therefore, additional effort is necessary to collect more  $V_s$  data from the gravel liquefaction sites to improve the existing  $V_s$ -based liquefaction triggering curves for gravelly soils.

#### 4. Collection of Additional Field Case History Data

In the present study, a larger database consisting of 174  $V_s$  data points and 137 DPT data points has been compiled by collecting additional data points from seven different countries around the world where gravel liquefaction did or did not take place in 17 major earthquake events and adding them to the existing data points from China reported by Cao et al. [21, 39]. Case histories with no liquefaction in Italy, Greece, and New Zealand were strategically identified, tested, and then added to the database to help constrain the position of the liquefaction triggering curves.

For each case history, the cyclic stress ratio (CSR) has been obtained by using the simplified equation

$$CSR = 0.65 (a_{max}/g) (\sigma_{vo}/\sigma'_{vo}) r_d \quad (1)$$

originally developed by Seed and Idriss [47] where  $a_{max}$  is the peak ground acceleration,  $\sigma_{vo}$  is the initial vertical total stress,  $\sigma'_{vo}$  is the initial vertical effective stress, and the  $r_d$  value in Eq. 1 was updated to include the effect of both depth and earthquake magnitude using the equation

$$r_d = e^{[\alpha(z)+\beta(z)M_w]} \quad (2)$$

where:

$$\alpha(z) = -1.012 - 1.126 \sin(z/11.73 + 5.133) \quad (3)$$

$$\beta(z) = 0.106 + 0.118 \sin(z/11.28 + 5.142) \quad (4)$$

and  $z$  is the depth in meters, based on the work by Golezorkhi [48] and Idriss [49].

Peak ground accelerations (*PGA* or  $a_{max}$ ) for every location were taken from the literature or from USGS Shake Maps [50] where necessary as employed by Idriss and Boulanger [51] for their CPT database. Besides *CSR*, the moment magnitude ( $M_w$ ) has been considered as another independent seismic variable for obtaining the liquefaction potential of gravelly soils. Values of  $M_w$  were found from available references regarding the appropriate earthquake. The data set contains a wide distribution of  $M_w$  ranging from 5.3 to 9.2 as well as *PGA* ranging from 0.17 to 0.6 g.

##### 4.1 DPT Blow Count Corrections

The DPT blow count,  $N_{120}$ , represents the number of hammer blows to drive the penetrometer 30 cm deep with a 120 kg hammer dropped from a height of 1 m. Raw blow counts are typically reported at every 10 cm penetration, but are multiplied by three to get the equivalent  $N_{120}$  for 30 cm of penetration.

Based on 1200 hammer energy measurements, Cao et al. [52] found that the Chinese DPT provided an average of 89% of the theoretical free-fall energy. Since the energy delivered by a given hammer ( $E_{\text{Hammer}}$ ) was different than the energy actually supplied by a Chinese DPT hammer ( $E_{\text{Chinese DPT}}$ ), it was sometimes necessary to correct the measured blow count. In this study, the correction was made using the simple linear reduction suggested by Seed et al. [53] for SPT testing

$$N_{120} = N_{\text{Hammer}} \cdot (E_{\text{Hammer}}/E_{\text{Chinese DPT}}) \quad (5)$$

where  $N_{\text{Hammer}}$  is the number of blows per 0.3 m of penetration obtained with a hammer delivering an energy of  $E_{\text{Hammer}}$ . In addition, Cao et al. [21] recommend an overburden correction factor,  $C_n$ , to obtain the normalized  $N'_{120}$  value using the equation

$$N'_{120} = N_{120} C_n \quad (6)$$

where

$$C_n = (100/\sigma'_{vo})^{0.5} \leq 1.7 \quad (7)$$

and  $\sigma'_o$  is the initial vertical effective stress in  $\text{kN/m}^2$ . In the current study, a limiting value of 1.7 was added to be consistent with the  $C_n$  used to correct penetration resistance from other in-situ tests [37]. For each case history a critical layer was selected below the water table and with the lowest ratio of blow count divided by CSR over at least one meter. All the critical liquefaction layers were located at depths less than about 14 m which is consistent with other liquefaction case history databases and with blow counts typically less than about 20.

## 4.2 DPT Blow Count Corrections

The  $V_s$  values obtained by various in-situ methods were corrected for overburden pressure to obtain  $V_{s1}$  using the equation:

$$V_{s1} = V_s (P_a/\sigma'_{vo})^{0.25} \quad (8)$$

where  $\sigma'_{vo}$  is the initial vertical effective stress, and  $P_a$  is atmospheric pressure approximated by a value of 100 kPa as suggested by Sykora [54] and adopted by Youd et al. [37]. These normalized  $V_{s1}$  profiles based on the  $V_s$  testing were then plotted as a function of depth and a critical depth with the lowest average ratio of  $V_{s1}/\text{CSR}$  over a length of at least one meter. Once again, the critical layers based on  $V_{s1}$  were all shallower than 14 m.

## 5. Development of Probabilistic Triggering Curves

Based on the new expanded database, a new set of probabilistic liquefaction triggering curves has been developed by logistic regression analysis based on  $V_{s1}$  and also  $N'_{120}$ . The triggering equations developed in the present study include the earthquake magnitude as an independent variable.

### 5.1 Probabilistic DPT-Based Liquefaction Triggering Curves

The logistical regression analysis was carried out using  $M_w$ ,  $N'_{120}$ , and  $\ln(\text{CSR})$  as independent variables and the following equation was developed to calculate the Cyclic Resistance Ratio (CRR)

$$\text{CRR} = \exp \left[ \frac{1.32M_w - 0.0008N'^3_{120} - \ln\left(\frac{1-P_L}{P_L}\right)}{5.2} \right] \quad (9)$$

where  $P_L$  is the probability of liquefaction expressed as a fraction. If a given probability and  $M_w$  of 7.5 is used in Eq. 9, a plot of  $\text{CRR}$  vs.  $N'_{120}$  can be produced for a given probability. Fig. 1 provides a plot of  $\text{CRR}$  vs.  $N'_{120}$  for  $M_w$  7.5 for various  $P_L$  values. CSR and  $N'_{120}$  data points for each liquefaction and no liquefaction case history are also shown in Fig. 1 relative to the triggering curves proposed by Rollins et al. [55].



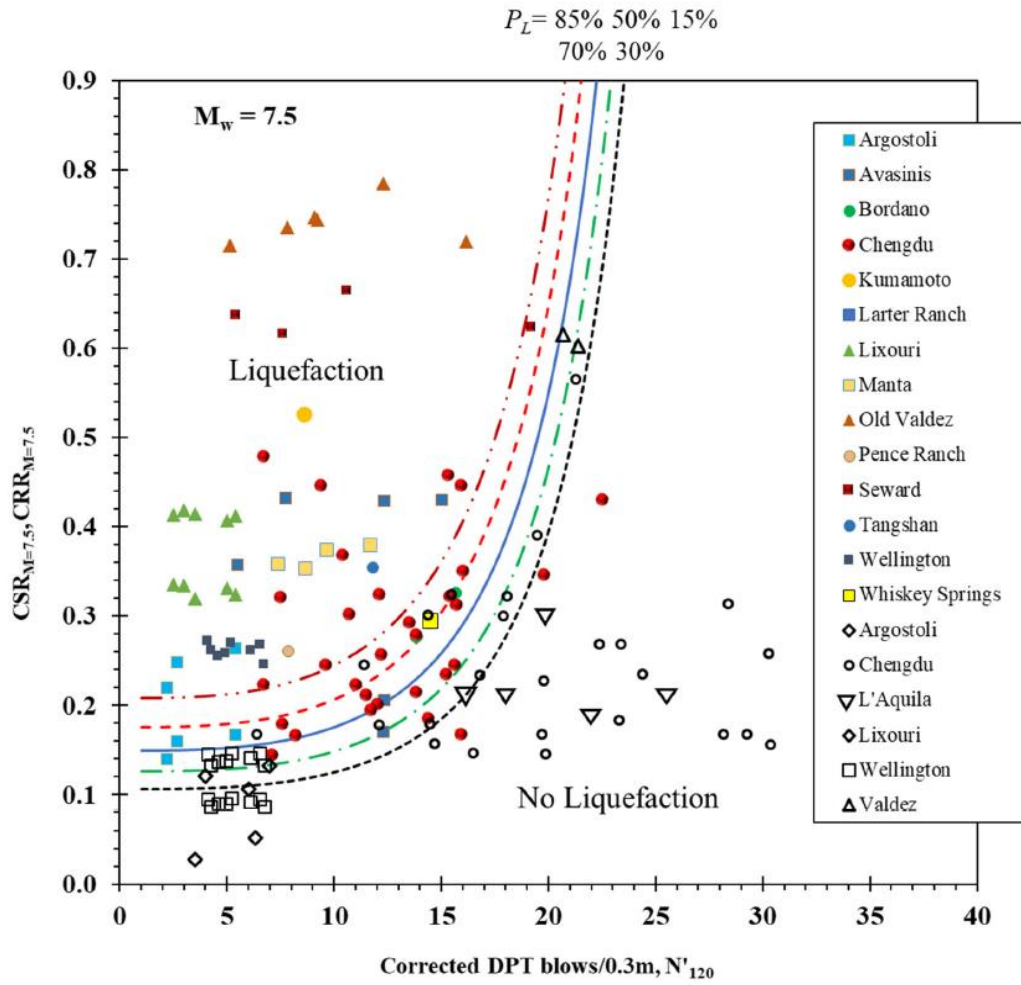


Figure 1. Plot of  $CRR$  vs.  $N'_{120}$  for a  $M_w$  7.5 earthquake with various probabilities of liquefaction based on expanded DPT-based database proposed by Rollins et al. [55].

## 5.2 Probabilistic $V_s$ -Based Liquefaction Triggering Curves

Logistical regression analysis was also carried out using  $M_w$ ,  $V_{s1}$  and  $\ln(CSR)$  as independent variables and the following equation was developed to calculate the Cyclic Resistance Ratio (CRR)

$$CRR = \exp \left[ \frac{1.438M_w - 3.8 \times 10^{-7} V_{s1}^3 - \ln \left( \frac{1-P_L}{P_L} \right)}{4.026} \right] \quad (10)$$

where  $P_L$  is the probability of liquefaction expressed as a fraction. If a given probability and  $M_w$  of 7.5 is used in Eq. 9, a plot of  $CRR$  vs.  $V_{s1}$  can be produced for a given probability. Fig. 2 provides a plot of  $CRR$  vs.  $N'_{120}$  for  $M_w$  7.5 for various  $P_L$  values proposed by Rollins et al. [56].

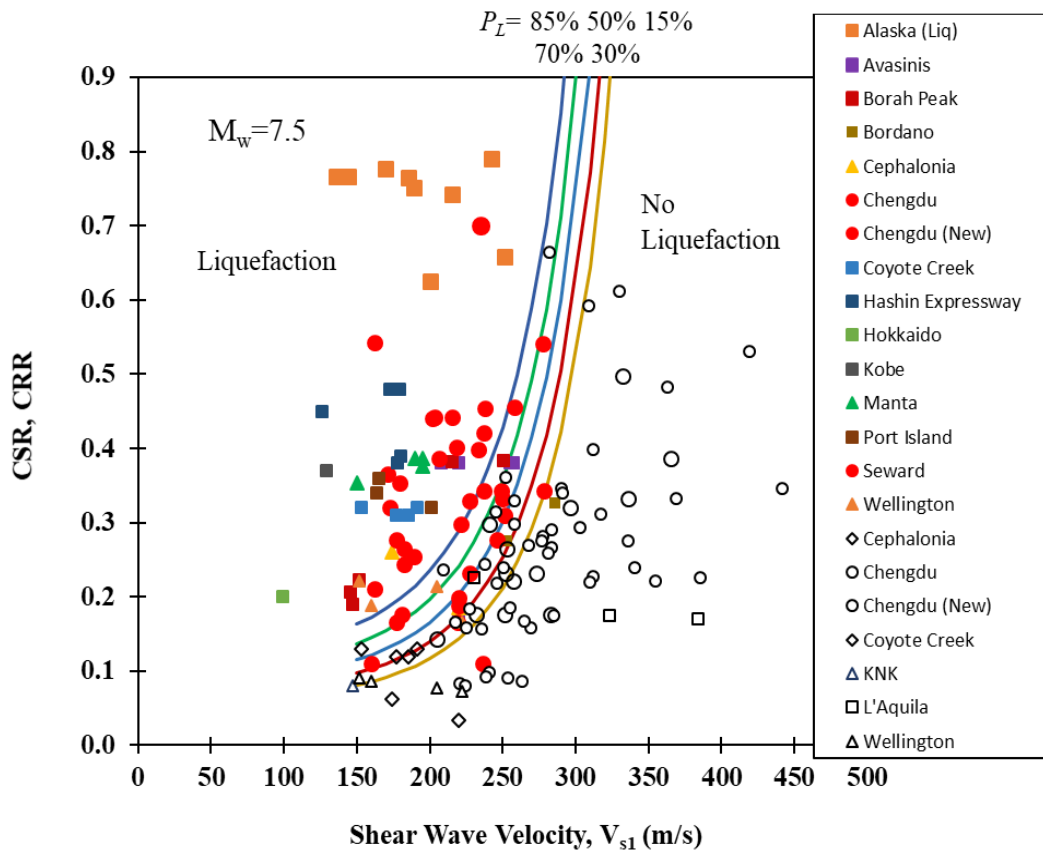


Figure 2. Plot of CRR vs.  $V_{s1}$  for a  $M_w$  7.5 earthquake with various probabilities of liquefaction based on expanded  $V_s$ -based database collected by Rollins et al. [56]

The new probabilistic triggering curves with liquefaction probabilities of 15% to 85% are plotted in Fig. 3(a) with solid lines along with similar curves developed by Cao et al. [46] with dashed lines to draw a distinct comparison between the two triggering procedures. For lower values of  $V_{s1}$  (around 150 m/s), the  $CRR$  for the new 50% probability of liquefaction curve is about 0.10 while it is only 0.04 for the Cao et al. [46] curves. This adjustment produces much better agreement with observed field performance. This higher  $CRR$  value at small velocities is also more typical of that predicted by the  $V_s$ -based triggering curves developed by Kayen et al. [38]. In fact, it can be seen from Fig. 3 that the points from the Port of Wellington where liquefaction did not take place during the Cook Strait and Lake Grassmere earthquakes (both  $M_w = 6.6$ ) in 2013 and the “no liquefaction” points from Argostoli, KNK and Coyote Creek have had a significant effect in constraining the lower branch of the triggering curves to move upwards. Likewise, the triggering curves at the higher range of  $V_{s1}$  values have been tightened relative to the curves developed by Cao et al. [46] as a result of the additional “no liquefaction” data points from Chengdu, L’Aquila and Valdez. Additional data points would certainly be desirable to define the shape of the curve better in this range of  $V_{s1}$  values.

In the middle range of the curve, a few “no liquefaction” points from the Chengdu plain fall above the 70% triggering curve and some liquefaction points from the same region fall below the 30% triggering curve. These points may belong to the false negative or false positive categories leading to inconsistent evaluation of the actual incident. Due to the presence of these points, the set of triggering curves develop a slightly sloped shape above a  $V_{s1}$  value of 200 m/s such that a number of “no liquefaction” points fall marginally on the 30% triggering curve instead of falling distinctly below this line.

As shown in Fig. 3(a), for  $V_{s1}$  values above 200 m/s, the  $P_L = 50\%$  curve for the new regression is very similar to that for the Cao et al. [46] regression. However, the addition of new liquefaction points has pulled the new  $P_L=85\%$  curve to the right while the addition of no-liquefaction data points has pulled

the new  $P_L=15\%$  curve to the left, relative to the Cao et al. [46] curves. Moving the new  $P_L=15\%$  curve to the left is particularly significant because this curve is often recommended for deterministic evaluations [38]. However, the slope of the new set of curves from this study remains almost the same as for the Cao et al. [46] curves. Overall, the spread between the triggering curves for various probabilities of liquefaction is substantially reduced for the new triggering curves relative to the Cao et al. [46] curves. This result is consistent with the concept that the increased number of data points reduces the uncertainty that develops when an individual data point plots in an unexpected position. Furthermore, the addition of data points where liquefaction did not occur has helped constrain the triggering curves on the “no liquefaction side” in critical locations.

A comparison is provided between the newly developed triggering curves for gravel and the curves developed by Kayen et al. [38] for sand in Fig.3(b). To plot the triggering curves for Kayen et al. [38], an average effective vertical stress of 100 kPa, and fines content of 6% has been assumed to keep the values within a reasonable range. Although the probabilistic liquefaction triggering curves for gravel developed in this study are similar to those for sands [38] at lower  $V_{s,1}$  values typical of looser gravels, the curves diverge as  $V_{s,1}$  increases. For example,  $V_{s,1}$  equals 275 m/s for the proposed  $P_L = 50\%$  curve for gravel in this study at a CRR of 0.5 in comparison with a  $V_{s,1}$  of only 225 m/s for the  $P_L = 50\%$  curve for sand proposed by Kayen et al. [38]. This indicates that the probabilistic triggering curves for gravels from this study shift to the right relative to similar curves developed for sands as  $V_{s,1}$  increases. This result indicates that gravels can still liquefy at  $V_{s,1}$  values that would be high enough to preclude liquefaction in a sand. This does not mean that gravels are more or less likely to liquefy than sand, it simply means that for a comparable level of shaking, a higher  $V_{s,1}$  is necessary to obtain the same probability of liquefaction for a sandy gravel than a sand. This result is consistent with liquefaction case histories in gravels reported by several investigators [24, 39, 44, 55, 57] where  $V_s$ -based triggering curves for sands would have incorrectly predicted no liquefaction, as well as laboratory testing (e.g. [58, 59]).



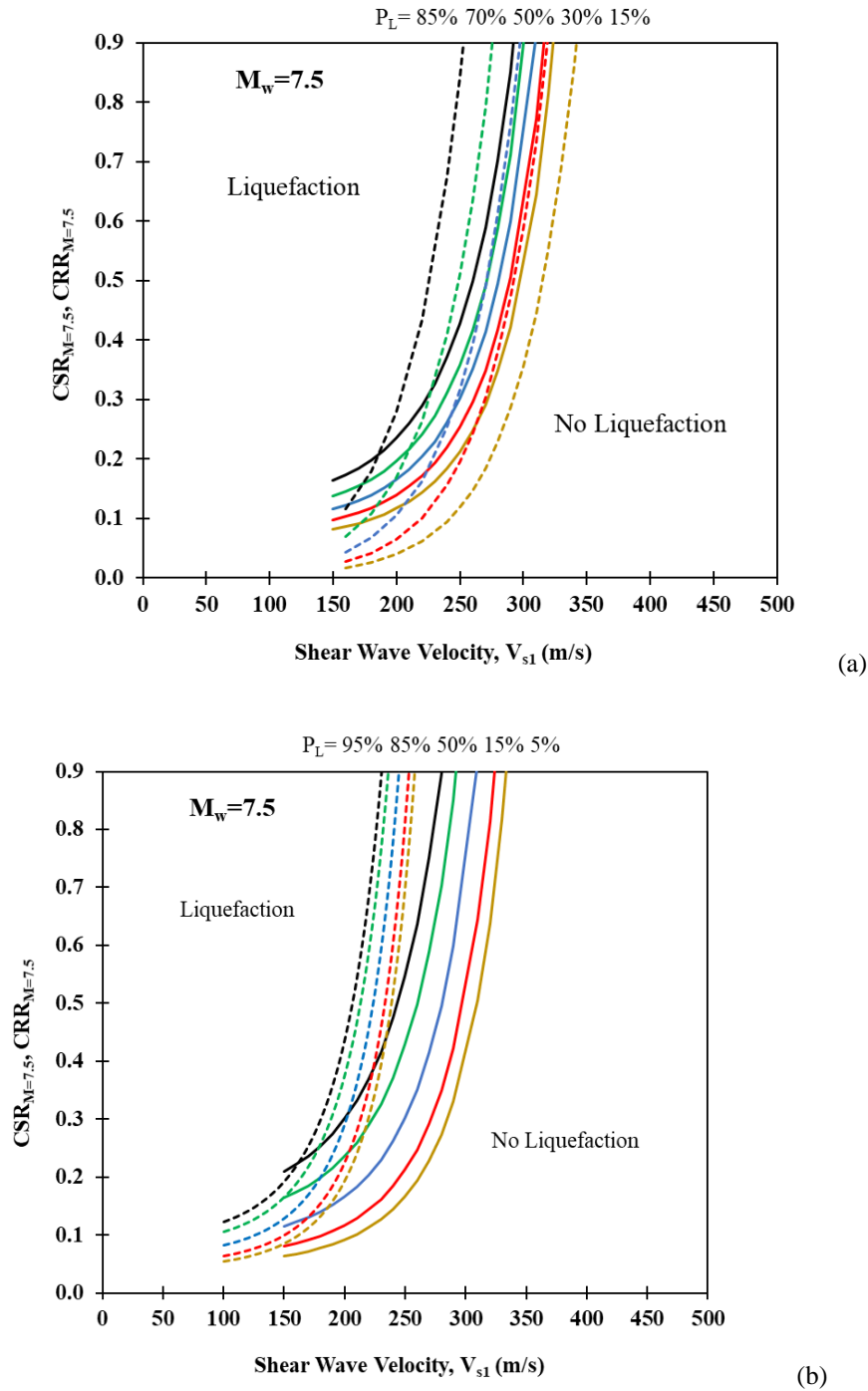


Figure 3. Revised liquefaction triggering curves from this study (solid lines) (a) relative to triggering curves originally proposed by Cao et al. [46] (dashed lines) and (b) relative to triggering curves proposed by Kayen et al. [38] for sands (dashed lines).

## 6. Development of Magnitude Scaling Factors

Most liquefaction triggering curves adjust the  $CSR$  for the earthquake magnitudes using a Magnitude Scaling Factor (MSF) to obtain an equivalent  $CSR$  for a  $M_w$  of 7.5 using the equation,

$$CSR_{M=7.5} = CSR/MSF \quad (11)$$

As a part of the present study, we have developed a new *MSF* models specifically for gravelly soils that may help improve liquefaction evaluation at some gravel sites, although more data from other earthquakes would be desirable. To obtain the *MSF*, *CSR* values were first obtained from Eq. 9 for  $M_w$  5.5 through 9 with an increment of 0.5 keeping  $N'_{120}$  and  $P_L$  constant. Then the *CSRs* for different magnitudes were divided by the *CSR* at  $M_w=7.5$  to obtain the magnitude scaling factor. The same process was then repeated by substituting different values of  $N'_{120}$  and  $P_L$  in Eq. 9 to obtain the variation of *MSF* with these variables. But notably, the *MSF* pattern did not show any variation with the DPT blow count ( $N'_{120}$ ) and the probability of liquefaction ( $P_L$ ). Based on this analysis the *MSF* for triggering analyses using the DPT blow counts can be computed as a function of magnitude with the best-fit exponential equation:

$$MSF = 7.258 \exp(-0.264M_w) \quad (12)$$

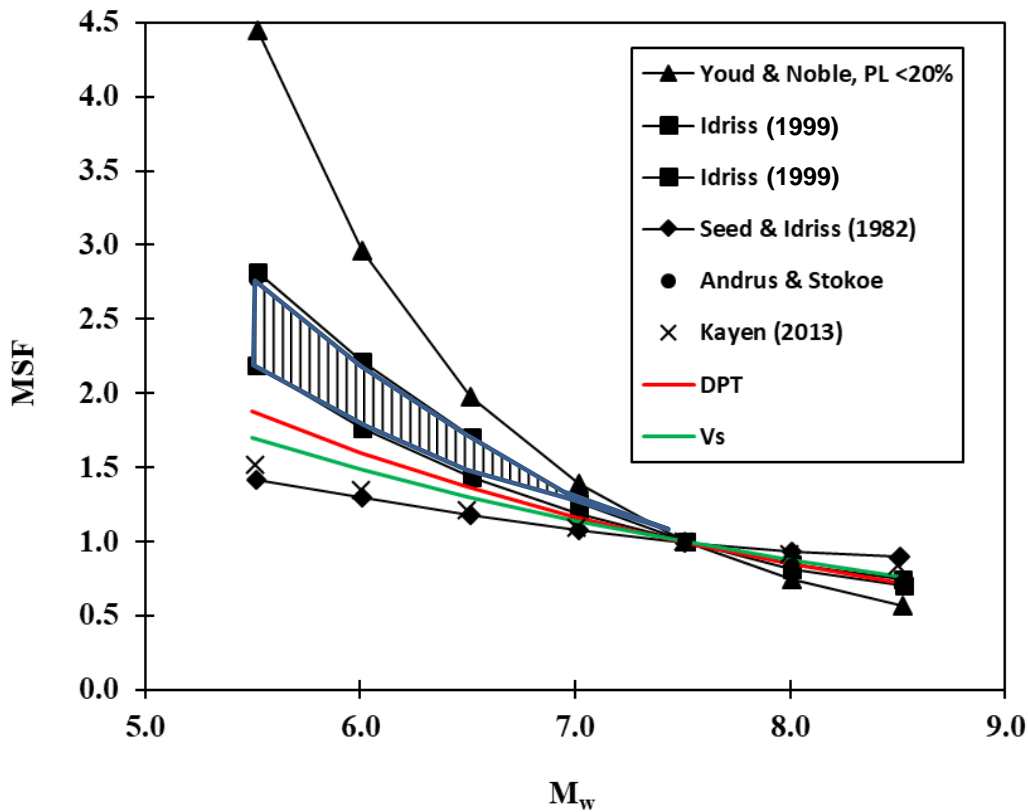


Figure 4. Comparison of *MSF* curves from logistical regression analysis of gravel liquefaction case histories based on *Vs* and DPT triggering curve with *MSF* curves proposed previously for sand [55, 56].

A similar approach was used to obtain the following best-fit exponential equation *MSF* equation for the *Vs*-based liquefaction triggering curve.

$$MSF = 10.667 \exp(-0.316M_w) \quad (13)$$

These *MSF* curves are plotted and compared with several other *MSF* vs.  $M_w$  curves in Fig. 4. It can be observed that the *MSF* curves developed for gravelly soil fall about mid-way between the *MSF* vs.  $M_w$  curves for sand suggested by Idriss as endorsed by the NCEER/NSF liquefaction workshop [37] at the high end and the Kayen et al. [38] curve at the low end. Hence, the proposed models for gravel appear to be reasonably consistent with existing *MSF* curves for sands.

Based on these *MSF* equations, the *CSRs* for all the case history data points have been converted to *CSRs* at  $M_w = 7.5$  and plotted with the newly developed triggering curves as shown in Figs. 1 and 2. Generally, the data points fall on the correct sides of the  $P_L = 50\%$  curves for the liquefaction and no liquefaction.

## 7. Summary and Conclusions

In this study, probabilistic liquefaction-triggering curves for gravelly soils based on the Dynamic Cone Penetration (DPT) test blow count ( $N'_{120}$ ) and shear-wave velocity ( $V_s$ ) were developed that can be used for liquefaction evaluation of gravelly soils for a wide range of earthquake magnitudes, tectonic settings, and geological environments. These curves are a significant step forward compared to those developed by Cao et al. [21, 39], as the total number of data points increased significantly. The  $N'_{120}$  and  $V_{s1}$  data were compiled from various sites around the world where liquefaction or no liquefaction case histories of gravelly soils were observed during several earthquake events in the past. The expanded data set consisted of 174  $V_s$  data points and 137 DPT data points from 17 different earthquakes in 10 different countries in a variety of geological environments.

Based on the results of the field studies and data analysis performed in this study, the following conclusions were drawn:

1. The increased number of liquefaction and no-liquefaction data points in the expanded data set better constrain the probabilistic liquefaction-triggering curves. Relative to the Cao et al. [46] curves for  $V_s$  and the Cao et al. [21] curves for DPT, this shifted the  $P_L = 85\%$  curve to the right and  $P_L = 15\%$  curve to the left. The reduction in the range between the  $P_L = 85\%$  and  $15\%$  curves indicate a considerable decrease in uncertainty, because false negative data points have less impact on the expanded data set. Shifting the  $P_L = 15\%$  curve to the left is significant because this probability curve has been recommended for deterministic analyses (e.g. [38]).
2. At lower  $V_{s1}$  values ( $\approx 150$  m/s) and DPT blow counts less than 7, typical of looser gravels, the proposed triggering curves for gravel in this study start at a higher range of CSRs compared to the curves developed by Cao et al. [21, 46]. This modification was necessary to produce agreement with the no-liquefaction points from the field case histories and brought the CSR values in line with the  $V_{s1}$  value for sand as predicted by the Kayen et al. [38] probability curves.
3. Simplified  $MSF$  versus moment magnitude  $M_w$  equations were developed exclusively for gravel liquefaction. The  $MSF$  versus  $M_w$  curves plot about midway between similar curves proposed for sand. These results suggest that the effect of magnitude on liquefaction resistance is similar, but slightly different, for both sands and sandy gravels.
4. Although the probabilistic triggering curves for gravel are similar to those for sands [38] at low  $V_{s1}$  values typical of loose gravels ( $\approx 150$  m/s), they shift to the right as  $V_{s1}$  values increase. This indicates that gravels can still liquefy at values that would preclude liquefaction for sands. Therefore, using  $V_s$ -based triggering curves for sand when encountering gravels could incorrectly estimate gravel susceptible to liquefaction as being non-liquefiable.

## Acknowledgements

Funding for this study was provided by grant G16AP00108 from the US Geological Survey Earthquake Hazard Reduction Program and grants CMMI-1663546 and CMMI- 1663288 from the National Science Foundation. This funding is gratefully acknowledged. This work is also part of a Research Project funded by ReLUIIS (University Network of Seismic Engineering Laboratories) Consortium 2019-2021, WP 16 Geotechnical Engineering, Task 16.1 Site response and liquefaction. However, the opinions, conclusions and recommendations in this paper do not necessarily represent those of the sponsors. We also express sincere appreciation to L. Minarelli for help in arranging access for geophysical surveys at sites in Italy and to G. Athanasopoulos for arranging access for these tests at sites in Cephalonia, Greece.

## References

- [1] Tokimatsu, K., and Yoshimi, Y. 1983. "Empirical correlation of soil liquefaction based on SPT N-value and fines content." *Soils and Foundations*, 23(4), 56-74.
- [2] Youd, T.L. and Hoose, S.N. 1978. "Historic ground failures in Northern California triggered by earthquakes." *U.S. Geological Survey Professional Paper 1993*, 180 p.
- [3] Baratta, M., 1910. *La Catastrofe Sismica Calabro-Messinese (28 dicembre 1908)*. Roma: Società Geografica Italiana.
- [4] Ishihara, K. 1985. "Stability of natural deposits during earthquakes." *Proc., 11th Int. Conf. on Soil Mech. and Found. Eng.*, 1, 321-376.
- [5] Coulter, H.W., and Migliaccio, R.R. 1966. "Effect of the Earthquake of March 22, 1964 at Valdez, Alaska." *U.S. Geological Survey Professional Paper 542-C*.
- [6] McCulloch, D. S., & Bonilla, M. G. 1970. "Effects of the earthquake of March 27, 1964, on the Alaska Railroad". US Government Printing Office.
- [7] Wang, W.S. 1984. "Earthquake damages to earth dams and levees in relation to soil liquefaction and weakness in soft clays." *In Proc. Intl. Conf. on Case Histories in Geotech. Eng.*, 1, 511-521.
- [8] Wang, W.S. 1984. "Earthquake damages to earth dams and levees in relation to soil liquefaction and weakness in soft clays." *In Proc. Intl. Conf. on Case Histories in Geotech. Eng.*, 1, 511-521.
- [9] Sirovich, L., 1996a. "Repetitive Liquefaction at gravelly site and liquefaction in overconsolidated sands." *Soils and Foundations*, (36)4, 23-34.
- [10] Sirovich, L., 1996b. "In-situ testing of repeatedly liquefied gravels and liquefied overconsolidated sands." *Soils and Foundations*, (36)4, 35-44.
- [11] Rollins, K.M., Amoroso, S., Milan, G., Minerelli, L., Vassallo, M., Di Giulio, G. 2020. "Gravel liquefaction assessment using the dynamic cone penetration test based on field performance from the 1976 Friuli earthquake." *J. Geotech. and Geoenviron. Eng.*, ASCE, [https://DOI.org/10.1061/\(ASCE\)GT.1943-5606.0002252](https://DOI.org/10.1061/(ASCE)GT.1943-5606.0002252),
- [12] Youd, T.L., Harp, E.L., Keefer, D.K., and Wilson, R.C. 1985. "The Borah Peak, Idaho Earthquake of October 29, 1983-Liquefaction." *Earthquake Spectra*, 2, 71-90.
- [13] Andrus, R.D. 1994. "In situ characterization of gravelly soils that liquefied in the 1983 Borah Peak earthquake." *Ph.D. Dissertation*, Civil Engineering Dept., Univ. of Texas at Austin, 579 pp.
- [14] Harder, L.F., Jr., and Seed, H.B. 1986. "Determination of penetration resistance for coarse-grained soils using the Becker Hammer Drill." College of Engineering, University of California, Berkeley, Calif. Rep. No. UCB/EERC-86/06. May 1986.
- [15] Yegian, M.K., Ghahraman, V.G., and Harutiunyan, R.N., 1994. "Liquefaction and embankment failure case histories, 1988 Armenia earthquake." *J. Geotech. Eng.*, 10.1061/(ASCE)0733-9410(1994)120:3(581).
- [16] Franke, K.W. and Rollins, K.M. 2017. "Lateral spread displacement and bridge foundation case histories from the 1991 M7.6 Earthquake near Limón, Costa Rica." *J. Geotechnical and Geoenvironmental Engineering*, ASCE, Vol. 143, No. 6, 17 p.
- [17] Maurenbrecher P.M., Den Outer, A., and Luger, H.J. 1995. "Review of geotechnical investigations resulting from the Roermond April 13, 1992 earthquake." *Proc. 3<sup>rd</sup> Int. Conf. on Recent Advances in Geotech. Earthquake Eng. and Soil Dyn.*, 645-652.
- [18] Kokusho, T., Tanaka, Y., Kudo, K., and Kawai, T., 1995. "Liquefaction case study of volcanic gravel layer during 1993 Hokkaido-Nansei-Oki earthquake." *Proc., 3<sup>rd</sup> Int. Conf. on Recent Advances in Geotech. Earthquake Eng. and Soil Dyn.*, 235-242.
- [19] Kokusho, T., and Yoshida, Y., 1997. "SPT N-value and S-wave velocity for gravelly soils with different grain size distribution." *Soils and Foundations*, 37(4): 105-113.
- [20] Chu, B.L., Hsu, S.C., Lai, S.E., and Chang, M.J. 2000. "Soil Liquefaction Potential Assessment of the Wu feng Area after the 921 Chi-Chi Earthquake." *Report of National Science Council* (in Chinese).

- [21] Cao, Z., Youd, T., and Yuan, X. 2013. "Chinese Dynamic Penetration Test for liquefaction evaluation in gravelly soils." *J. Geotech. Eng.*, 10.1061/(ASCE)GT.1943-5606.0000857.
- [22] Towhata (personal communication in 2016)
- [23] Nikolaou, S., Zekkos, D., Assimaki, D., and Gilsanz, R. 2014. "GEER/EERI/ATC Earthquake Reconnaissance January 26<sup>th</sup>/February 2<sup>nd</sup> 2014 Cephalonia, Greece Events, Version 1." [http://www.geerassociation.org/index.php/component/geer\\_reports/?view=geerreports&id=32](http://www.geerassociation.org/index.php/component/geer_reports/?view=geerreports&id=32)
- [24] Athanasopoulos-Zekkos, A., Zekkos, D., Rollins, K.M., Hubler, J., Higbee, J., Platis, A. 2019. "Earthquake performance and characterization of gravel-size earth fills in the ports of Cephalonia, Greece, following the 2014 Earthquakes." *Earthquake Geotechnical Engineering for Protection and Development of Environment and Constructions*, Procs. 7th Intl. Conf. on Earthquake Geotechnical Engineering, Taylor and Francis, p. 1212-1219.
- [25] Rollins, K.M., Ledezma, C., and Montalva, G., Becerra, A., Candia, G., Jara, D., Franke, K., Saez, E. 2014. *Geotechnical Aspects of April 1, 2014, M8.2 Iquique, Chile Earthquake.* GEER Association Report No. GEER-038, 77 p. Version 1.2: October 22, 2014
- [26] Morales, C., Ledezma, C., Saez, E., Boldrini, S., and Rollins, K.M., 2020. "Seismic failure of an old pier during the 2014 Mw8.2, Pisagua, Chile earthquake." *Earthquake Spectra*, EERI, <https://journals.sagepub.com/doi/10.1177/8755293019891726>
- [27] Sebastian Lopez, J. Vera-Grunauer, X., Rollins, K., and Salvatierra, G. 2018. "Gravelly Soil Liquefaction after the 2016 Ecuador Earthquake." *Procs. Geotechnical Earthquake Engineering and Soil Dynamics V*, 13 p.
- Seed, H. B., and Idriss, I. M. 1971. "Simplified procedure for evaluating soil liquefaction potential." *J. Geotech. Engrg. Div.*, ASCE, 97(9), 1249–1273.
- [28] Cubrinovski, M., Rhodes, A., Ntritsos, N., and Van Ballegooy, S. 2017. "System response of liquefiable deposits." *Proc., Performance Based Design III*, 18p.
- [29] Pavlides, S., Muceku, Y., Chatzipetrow, A., Georgious, G., Lazos, I. 2020. "Preliminary report on the ground failures of the Albanian (Durres-Thumane) 26<sup>th</sup> of November Earthquake,
- [30] Amoroso, S., Barbača, J., Belić, N., Kordić, B., Brčić, V., Budić, M., Civico, R., De Martini, P. M., Hećej, N., Kurečić, T., Minarelli, L., Novosel, T., Palenik, D., Pantosti, D., Pucci, S., Filjak, R., Ricci, T., Špelić, M., and Vukovski, M. 2021. Liquefaction field reconnaissance following the 29th December 2020 Mw 6.4 Petrinja earthquake (Croatia), EGU General Assembly 2021, online, 19–30 Apr 2021, EGU21-16584,
- [31] DeJong, J.T., Ghafghazi, M., Sturm, A.P., Wilson, D.W., den Dulk, J., Armstrong, R.J., Perez, A., and Davis, C.A. 2017. "Instrumented Becker Penetration Test. I: Equipment, Operation, and Performance." *J. Geotech. Eng.*, doi.org/10.1061/(ASCE)GT.1943-5606.0001718.
- [32] Harder, L.F., Jr., and Seed, H.B. 1986. "Determination of penetration resistance for coarse-grained soils using the Becker Hammer Drill." College of Engineering, University of California, Berkeley, Calif. Rep. No. UCB/EERC-86/06. May 1986.
- [33] Harder, L.F. 1997. "Application of the Becker Penetration Test for evaluating the liquefaction potential of gravelly soils." *NCEER Workshop on Evaluation of Liquefaction Resistance*, held in Salt Lake City, Utah.
- [34] ASTM. 2018. Standard test method for use of the dynamic cone penetrometer in shallow pavement applications. ASTM D6951/D6951M-18. West Conshohocken, PA: ASTM.
- [35] British Standard 2012, Geotechnical investigation and testing — Field testing — Part 2: Dynamic probing BS EN ISO 22476-2:2005+A1:2011
- [36] Boulanger, R.W. and Idriss, I.M. 2014. "CPT and SPT based liquefaction triggering procedures." Center of Geotechnical Modeling, Univ. of California-Davis, Report No. UCD/CGM-14/01.
- [37] Youd, T.L., Idriss, I.M., Andrus, R.D., Arango, I., Castro, G., Christian, J.T., Dory, R., Finn, W.D.L., Harder, L.F., Hynes, M.E., Ishihara, K., Koester, J.P., Liao, S.S.C., Marcuson, W.F., Martin, G.R., Mitchell, J.K., Moriwaki, Y., Power, M.S., Robertson, P.K., Seed, R.B., and Stokoe, K.H. 2001. "Liquefaction resistance of soils: Summary Report from the 1996 NCEER and 1998 NCEER/NSF Workshops on evaluation of liquefaction resistance of soils." *J. Geotech. Eng.*, 10.1061/(ASCE)1090-0241(2001)127:10(817).



- [38] Kayen, R., Moss, R.E.S., Thompson, E.M., Seed, R.B., Cetin, K.O., Der Kiureghian, A., Tanaka, Y., and Tokimatsu, K. (2013). "Shear-wave velocity-based probabilistic and deterministic assessment of seismic soil liquefaction potential." *J. Geotech. Eng.*, doi.org/10.1061/(ASCE)GT.1943-5606.0000743.
- [39] Stokoe, K. H. II, Wright, S. G., Bay, J. A., and Roesset, J. M. 1994. "Characterization of geotechnical sites by SASW method," ISSMFE, Technical Committee #10 for XIII ICSMFE, Geophysical Characterization of Sites, A. A. Balkema Publishers/Rotterdam & Brookfield, Netherlands, 15–25.
- [40] Andrus, R.D., and Stokoe, K.H., II 2000. "Liquefaction resistance of soils from shear-wave velocity." *J. Geotech. Eng.*, 10.1061/(ASCE)1090-0241(2000)126:11(1015).
- [41] Ohta, Y. and Goto, N. 1978. "Physical background of the statistically obtained S-wave velocity equation in terms of soil indexes." *ButsuriTanko(Geophysical Exploration)*, Tokyo, Japan, 31(1), 8-17 (In Japanese).
- [42] Rollins, K.M., Evans, M., Diehl, N. and Daily, W. 1998b. "Shear modulus and damping relationships for gravels." *J. Geotech. and Geoenviron. Eng.*, ASCE, 124(5) p. 396-405.
- [43] Weston, T. R. 1996. "Effects of grain size and particle distribution on the stiffness and damping of granular soils at small strains." MS thesis, University of Texas, Austin, Texas.
- [44] Chang, W.J. 2016. "Evaluation of liquefaction resistance for gravelly sands using gravel content-corrected shear-wave velocity." *J. Geotech. Eng.*, 10.1061/(ASCE)GT.1943-5606.0001427.
- [45] Chen, L. Yuan, X., Cao, Z. Sun, R. Wang, w., and Liu H. 2018. *Earthquake Spectra*, 34(3) p. 1091-1111
- [46] Cao, Z., Youd, T.L., and Yuan, X. 2011. "Gravelly soils that liquefied during 2008 Wenchuan, China Earthquake, Ms=8.0." *Soil Dynamics and Earthquake Engineering*, 31(8), 1132-1143.
- [47] Seed, H. B., and I. M. Idriss. 1971. "Simplified procedure for evaluating soil liquefaction potential." *J. Soil Mech. Found. Div.* 97 (9): 1249–1273 <https://doi.org/10.1061/JSFEAQ.0001662>.
- [48] Golesorkhi, R. 1989. "Factors influencing the computational determination of earthquake-induced shear stresses in sandy soils." PhD dissertation, University of California, Berkeley, California.
- [49] Idriss, I.M. 1999. "An update to the Seed-Idriss simplified procedure for evaluating liquefaction potential." *Procs. TRB Workshop on New Approaches to Liquefaction*, Publication No. FHWA-RD-99-165, Federal Highway Administration.
- [50] Worden, C. B., Wald, D. J., Allen, T. I., Lin, K., and Cua, G. 2010. "Integration of macroseismic and strong-motion earthquake data in ShakeMap for real-time and historic earthquake analysis." USGS website, <http://earthquake.usgs.gov/earthquakes/shakemap/>.
- [51] Idriss, I. and Boulanger, R. W. 2008. "Soil liquefaction during earthquakes." Earthquake Engineering Research Institute.
- [52] Cao, Z., Yuan, X., Youd, T.L., and Rollins, K.M. 2012. "Chinese Dynamic Penetration tests (DPT) at liquefaction sites following 2008 Wenchuan Earthquake." *Proc., 4th Int. Conf. on Geotechnical and Geophysical Site Characterization*, Taylor & Francis Group, London, 1499-1504.
- [53] Seed, H.B., Tokimatsu, K., Harder, L.F., and Chung, R.M. 1985. "Influence of SPT procedures in soil liquefaction resistance evaluations." *J. Geotech. Eng.*, 10.1061/(ASCE)0733-9410(1985)111:12(1425).
- [54] Sykora, D. W. 1987. "Creation of a data base of seismic shear wave velocities for correlation analysis." *Geotech. Lab. Misc. Paper GL-87-26*, U.S. Army Engr. Waterways Experiment Station, Vicksburg, Miss.
- [55] Rollins, K.M., Roy, J., Athanasopoulos-Zekkos, A., Zekkos, D., Amoroso, S., Cao, Z. (2021). "New dynamic cone penetration test-based procedure for liquefaction triggering assessment of gravelly soils." *J. Geotechnical and Geoenvironmental Engrg.* ASCE, 147(12), 13 p.
- [56] Rollins, K.M., Roy, J., Athanasopoulos-Zekkos, A., Zekkos, D., Amoroso, S., Cao, Z., Millana, G., Vassallo, M., Di Giulio, G. (2022). "A New  $V_s$ -Based Liquefaction Triggering Procedure for Gravelly Soils." *J. Geotechnical and Geoenvironmental Engrg.*, 148(6), 15 p. ASCE DOI: 10.1061/(ASCE)GT.1943-5606.0002784
- [57] Rollins, K.M., Amoroso, S., Milan, G., Minerelli, L., Vassallo, M., Di Giulio, G. (2020). "Gravel liquefaction assessment using the dynamic cone penetration test based on field performance from the 1976 Friuli earthquake." *J. Geotechnical & Geoenvironmental Engrg.*, ASCE, 146(6)

- [58] Hubler, J., Athanasopoulos-Zekkos, A., and Zekkos, D. 2018 “Monotonic and cyclic simple shear response of gravel-sand Mixtures”, *Soil Dynamics and Earthquake Engineering*, Vol 115, pp. 291-304, Dec 2018,
- [59] Hubler, J., Athanasopoulos-Zekkos, A., and Zekkos, D. 2017. “Monotonic, cyclic and post-cyclic simple shear response of three uniform gravels in constant volume conditions”, *J. Geotech. and Geoenviron Eng.* ASCE, Washington, DC, 143(9)